Title
Nanomechanical testing of freestanding polymer films: in situ tensile testing and Tg measurement

Journal
Journal of Materials Research, 36(12)

ISSN
0884-2914

Authors
Velez, Nathan R
Allen, Frances I
Jones, Mary Ann
et al.

Publication Date
2021-06-28

DOI
10.1557/s43578-021-00163-z

Peer reviewed

Journal of MATERIALS RESEARCH

Article
DOI:10.1557/s43578-021-00163-z

ADVANCED NANOMECHANICAL TESTING

FOCUS ISSUE

Nanomechanical testing of freestanding polymer films: in situ tensile testing and T_g measurement

Nathan R. Velez[1,2], Frances I. Allen[1,2], Mary Ann Jones[3], Jenn Donohue[1,2], Wei Li[4], Kristofer Pister[4], Sanjay Govindjee[5], Gregory F. Meyers[3], Andrew M. Minor[1,2,a)]

[1] Department of Materials Science and Engineering, UC Berkeley, Berkeley, CA 94720, USA
[2] National Center for Electron Microscopy, LBNL, Molecular Foundry, Berkeley, CA 94720, USA
[3] Core R&D - Analytical Sciences, The Dow Chemical Company, Midland, MI 48667, USA
[4] Department of Electrical Engineering and Computer Science, UC Berkeley, Berkeley, CA 94720, USA
[5] Department of Civil and Environmental Engineering, UC Berkeley, Berkeley, CA 94720, USA
[a)] Address all correspondence to this author. e-mail: aminor@berkeley.edu

Received: 2 December 2020; accepted: 9 March 2021; published online: 2 April 2021

A method for small-scale testing and imaging of freestanding, microtomed polymer films using a push-to-pull device is presented. Central to this method was the development of a sample preparation technique which utilized solvents at cryogenic temperatures to transfer and deposit delicate thin films onto the microfabricated push-to-pull devices. The preparation of focused ion beam (FIB)-milled tensile specimens enabled quantitative in situ TEM tensile testing, but artifacts associated with ion and electron beam irradiation motivated the development of a FIB-free specimen preparation method. The FIB-free method was enabled by the design and fabrication of oversized strain-locking push-to-pull devices. An adaptation for push-to-pull devices to be compatible with an instrumented nanoindenter expanded the testing capabilities to include in situ heating. These innovations provided quantitative mechanical testing, postmortem TEM imaging, and the ability to measure the glass transition temperature, via dynamic mechanical analysis, of freestanding polymer films. Results for each of these mentioned characterization methods are presented and discussed in terms of polymer nanomechanics.

Introduction

Small-scale mechanical testing methods offer many advantages over their macroscopic counterparts. The mechanical properties of materials often depend on mechanisms operating at length scales spanning several orders of magnitude. By reducing the size of the test specimen, features of interest can be isolated and measured independently. For example, single crystal plasticity can be studied for complex alloys [1–3], or near specific grain boundary structures [4]. Small-scale testing also provides a means to study size effects in materials in which one or more dimensions have been reduced to the micro- or nano-scale, for example as in nanopillar compression testing [5]. Another motivation for small-scale testing methods is to investigate materials that are inherently small such as nanowires [6], thin films [7], and biological specimens [8]. Finally, the powerful imaging and analytical capabilities of transmission electron microscopy (TEM) can be used to characterize materials if they are thin enough to be electron transparent. As will be elaborated upon, TEM can also be combined with mechanical testing platforms to enable in situ and postmortem experiments, specifically through the use of push-to-pull (PTP) devices (Fig. 1) [9, 10].

In polymeric materials, the prevailing method for thin-film preparation is spin-casting. This requires the polymer to be dissolved in a solvent, which is incompatible with many polymer systems of interest such as polymer blends, polymer composites, and highly immiscible polymers. A key advantage of our technique is the variety of samples that can be tested in tension, including films that are microtomed from bulk that contain composite particles or phase interfaces to be preserved.

This paper details the advantages and disadvantages of PTP-based methods for small-scale mechanical testing of freestanding, microtomed polymer thin films. The development of these methods has led to the discovery of a previously unknown phenomenon in thin films of polystyrene (PS) and

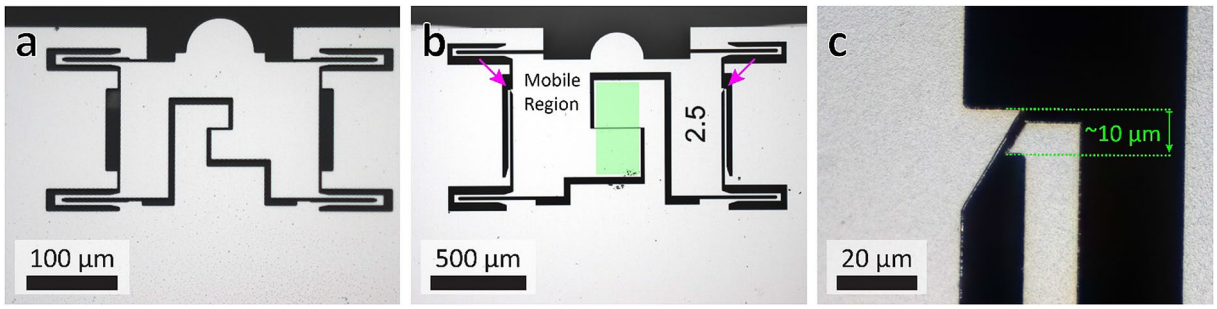

Figure 1: (a) Optical image of a commercially available (non-locking) PTP device. (b) Optical image of an oversized PTP device with custom-designed strain-locking mechanisms incorporated into the device (indicated by arrows). The locking PTP device is shown here with a 2.5 µm tensile gap and the green shaded area represents the region in which a specimen can be deposited without requiring FIB milling. (a, b) Both PTP devices are actuated by an in-plane force applied to the rounded top portion of the mobile region, which is suspended by four springs. Upon actuation, the horizonal gap in the center is widened to impart a tensile force on a specimen spanning the gap. (c) Close-up image of one of the two strain-locking mechanisms from (b). The minimum displacement (~10 µm) required to engage the strain-locking mechanism is annotated.

polymethylmethacrylate (PMMA), where it was found that the fractured surfaces imparted by microtomy can lead to extreme ductility in polymers which are otherwise known to be brittle in their bulk form [11–14]. As a result, even though microtomy is established as a standard sample preparation method for microscopy of polymers, it is clear that the mechanical properties of freestanding thin films prepared in this way can deviate significantly from their bulk counterparts.

Results and discussion

FIB-Milled tensile specimens

Employing the cryo-solvent manipulation technique (see Materials and Methods section), microtomed films of PS were deposited onto non-locking, commercially available PTP devices (Fig. 2a). It was not possible to prepare films with in-plane dimensions small enough such that material did not extend beyond the tensile region, hindering proper actuation of the PTP device. Thus, FIB milling was used to remove excess material and shape the tensile specimen.

Despite the precautions taken to avoid electron and ion beam exposure of the tensile specimen, unavoidable ion beam damage was present at the milled edges of the dogbone. Ion irradiation of polymers is known to cause chain scission of the carbon backbone and may subsequently produce radicals [15]. This can induce crosslinking through new bond formations between neighboring polymer chains. Additionally, scattered ions may embed into the polymer and, due to the low thermal conductivity of polymers, may cause local heating to occur [16]. Attempts to minimize these effects included using the FIB to widen the

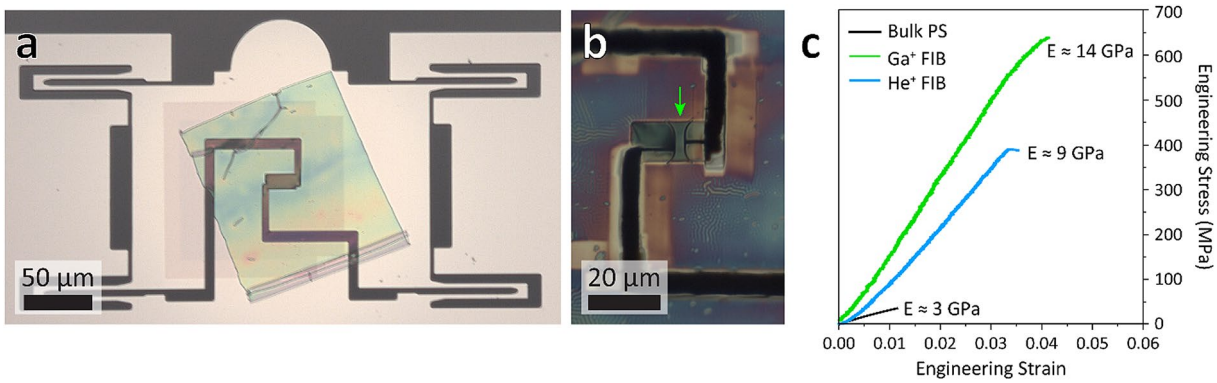

Figure 2: (a) Microtomed film (270 nm thick) of an elastomer deposited onto a commercial PTP device with a tensile gap that has been FIB milled to be ~11 µm instead of the standard 2.5 µm. (b) FIB-milled tensile specimen with a dogbone geometry (indicated by arrow). The surrounding wrinkling pattern was induced through ion beam exposure, which was not present at the tensile specimen to indicate that proper precautions were taken to avoid exposure during the FIB milling process. The dogbone shown was 280 nm thick and 2.3 µm wide. (c) Comparison of the mechanical responses for PS tensile specimens: microtomed film with a gallium FIB-milled dogbone (green curve), microtomed film with a helium FIB-milled dogbone (blue curve), and an injection-molded bulk PS dogbone (black curve). While helium ion milling offers some improvement, the mechanical response is still significantly altered by the irradiation damage at the edges, likely enhanced due to sample drift during the longer milling times. The thicknesses for the gallium and helium FIB-milled PS films were 330 and 140 nm, and the widths 13.5 and 0.8 µm, respectively. The strain rate used in the bulk tensile test was 0.01 s^{-1} and 0.0008 s^{-1} for the PTP tests.

tensile gap of the PTP device, so that larger tensile specimens could be prepared. This was to reduce the volume fraction of material exposed to ion irradiation. Additionally, FIB milling using a helium ion microscope, rather than the typical gallium FIB, was employed to reduce ion implantation at the edges due to the much larger stopping distance of the light ions [17]. However, despite our best efforts during the FIB preparation, the mechanical response of the polymer films tested in this manner was dominated by the ion-irradiated edges. As shown in Fig. 2, FIB-milled PS films led to stiffening that resulted in an elastic modulus up to three times larger than that of bulk tensile specimens, likely due to FIB-induced crosslinking at the edges. This was the case even when the width of the dogbone was increased to 13.5 μm (nearly spanning the entire width of the tensile gap), to reduce the volume fraction of the irradiated edges. Thus, in order to obtain meaningful quantitative measurements a FIB-free sample preparation technique was employed.

FIB-Free tensile specimens

As mentioned, a microtomed film could not be prepared small enough such that it would not extend beyond the tensile gap. This prompted the design and fabrication of larger PTP devices with a tensile region wide enough to deposit a microtomed film without the need for any FIB milling (Fig. 1b). The new design also incorporated a strain-locking mechanism which allowed the tensile gap to be held open for postmortem imaging, by either TEM or optical microscopy (Fig. 1c). Standard bulk silicon microfabrication was used to produce the oversized locking PTP devices. The smallest feature size was limited to about 2 μm using standard photolithography in contact mode. Because of this limitation, a minimum displacement of roughly 10 μm was required for the strain-locking mechanism to reach the locked position of the device (Fig. 1c). Thus, various tensile gap sizes were fabricated to predetermine the amount of strain that would be held in the locked position. Using the cryo-solvent manipulation method described in the Materials and Methods section and the newly designed locking PTP devices, microtomed polymer films could be deposited across the tensile gap without extending beyond the width of the tensile region (Fig. 3a, b). This avoided the need for FIB milling and the accompanying artifacts. As a result, it was discovered that microtomed PS becomes extremely ductile compared to bulk tensile tests due to the microtoming causing an effect analogous to mechanical rejuvenation, as discussed in prior work [11].

In situ TEM mechanical testing

The original design intent of the commercial PTP device was to enable in situ TEM mechanical testing [9]. This was performed by mounting the device into a specialized TEM holder equipped with an indenter capable of depth and force sensing (Bruker-Hysitron PI 95). This provided the means to acquire the mechanical response of the material with correlated TEM imaging. The cryo-manipulation method enabled in situ TEM mechanical testing of polymer films (Fig. 4, Video S1). Quantitative analysis, however, is limited by the damaging effects of the electron beam. Similar to ion beam irradiation, the electron beam inflicts localized heating and radiolysis in polymers that significantly alter their mechanical properties [18]. As shown in Fig. 4c, the stress–strain curves for an elastomer are dramatically affected by the electron beam during in situ testing compared to PTP testing with the electron beam off. These effects were expected to affect PS and PMMA similarly and so alternative characterization methods were explored, as discussed below. Therefore, the beam sensitivity of the material must be considered when attempting to acquire quantitative, in situ TEM mechanical data.

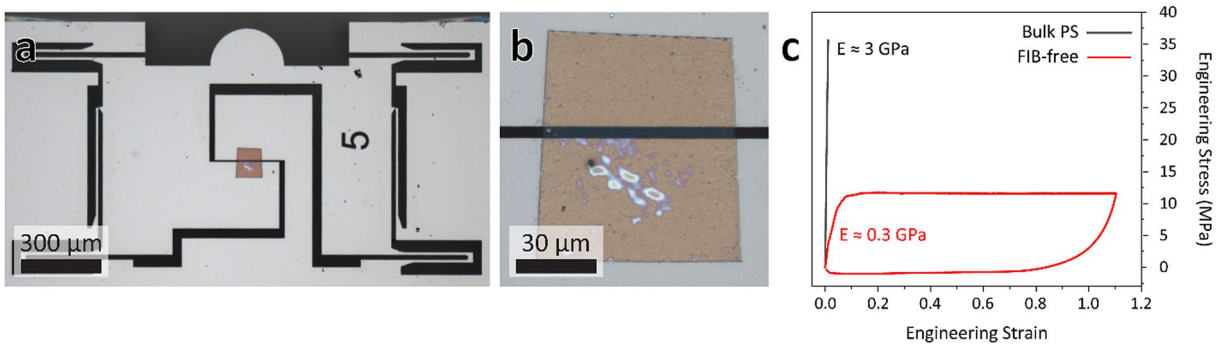

Figure 3: (a) Microtomed film (230 nm thick) of PMMA deposited onto an oversized locking PTP device with a tensile gap of 5 μm using the cryo-solvent manipulation technique. (b) Magnified image of the same film shown prior to mechanical testing (postmortem image shown in Fig. 6(e). (c) Comparison of the mechanical responses for a bulk, injection-molded tensile specimen (black curve) and a microtomed, FIB-free specimen (red curve) of PS. By avoiding the artifacts induced by ion and electron beam irradiation, the discovery of extreme ductility in microtomed films of PS was made possible through FIB-free specimen preparation (note that fracture did not occur). The thickness of the FIB-free film of PS was 450 nm, with a strain rate of 0.03 s^{-1} used during the PTP test.

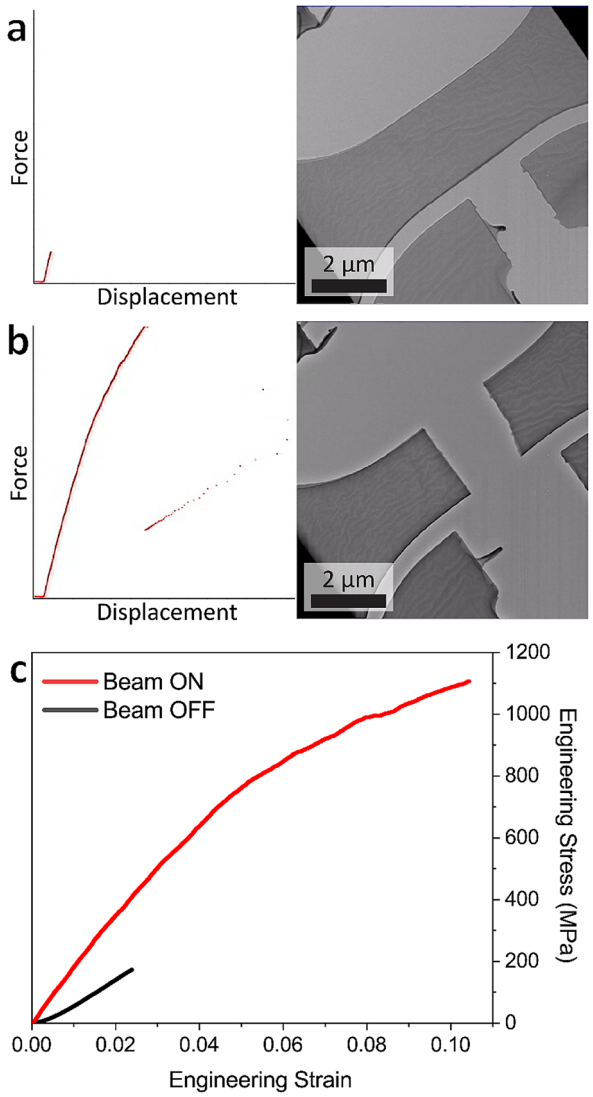

Figure 4: (a) and (b) Video snapshots from an in situ TEM tensile test with correlated force–displacement curve of a microtomed elastomer film, FIB milled into a dogbone geometry. (a) Snapshot from the beginning of the test. (b) Snapshot just after the specimen fractured. (c) Resultant stress–strain curve for the in situ test shown (red) in comparison to an identically prepared specimen in which the electron beam was blanked during the test (black). The stark difference between these two results highlights the sensitivity many polymeric materials have to the electron beam of the TEM (300 kV JEOL 3010). The thicknesses for these two films were 300 and 270 nm for the in situ test and 'blind' test, respectively (See SI for video.).

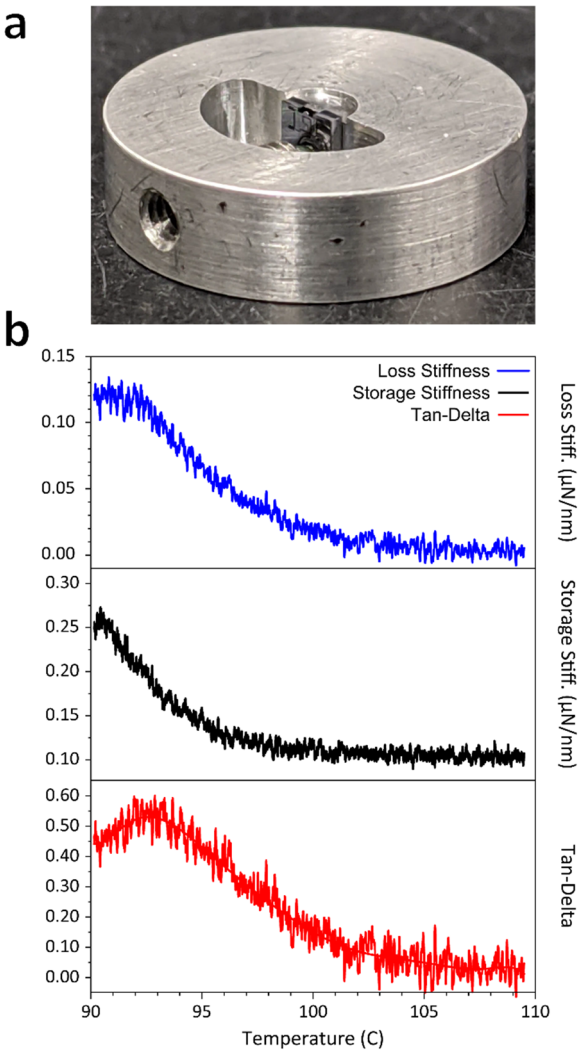

Figure 5: (a) Custom-fabricated mount designed to hold a locking PTP device upright for testing with an instrumented nanoindenter (different sized mount was also fabricated for the commercial PTP devices). A set screw with a nylon tip holds the device firmly in the vertical position. The top surface of the mount is slightly higher than the device, which allows it to be sandwiched between two heating plates for temperature-controlled testing. (b) Plot showing the results of a temperature-controlled DMA test on a microtomed, FIB-free film of PS. The thickness of the film was 140 nm, and the dynamic mechanical test was performed at 4 Hz with a continuous temperature increase at a rate of 4 °C/min.

Adaptation for quantitative testing with a nanoindenter

Since our locking PTP devices allow for larger tensile specimens, larger loads are required to strain these specimens. Because of this, the load limit for the indenting TEM holder was often exceeded. To overcome this limitation, a mount was designed to fix the locking PTP vertically, enabling the use of an instrumented nanoindenter (Bruker-Hysitron TI 950 TriboIndenter) to perform quantitative testing (Fig. 3c). Not only can this adaptation allow larger loads to be reached, but it extended all testing capabilities of the nanoindenter to both PTP and locking PTP devices that were not available with an indenting TEM holder. This includes the ability to perform temperature-controlled dynamic mechanical analysis (DMA) testing to measure the glass transition temperature of the freestanding polymer thin films (T_g). As shown in Fig. 5, T_g could be determined by measuring the storage and loss stiffness, providing a tan-delta value as a function of temperature [19]. As determined by the peak

in the tan-delta curve, the microtomed freestanding film of PS appears to have a reduction in T_g as compared to bulk measurements. This is expected due to the enhanced chain mobility at the microtomed surfaces [11], but further investigation is required to validate the repeatability of this result (T_g of bulk PS is 100 °C).

In Situ optical microscopy with postmortem TEM imaging

To avoid electron beam-induced artifacts, locking PTP experiments can be performed under an optical microscope to observe the deformation in situ. This can be done by fixing a pair of self-closing tweezers to the stage of an optical microscope to hold the locking PTP device under the objective lens (Fig. 6a). By equipping a micromanipulator setup with a needle, the locking PTP device can be actuated while recording optical video or images (Fig. 6b, Video S1). After applying enough displacement to engage the strain-locking mechanism, the locking PTP can then be transferred into the TEM holder for postmortem TEM imaging (Fig. 6c). The strain-locks provide more stability compared to holding strain with the indenting TEM holder, and even allow for the sample to be sputter coated in the deformed state to reduce electron beam sensitivity; both of these factors enhance the ability to obtain high-quality TEM images postmortem.

Conclusion

The PTP-based mechanical testing platform, which has had success in studying hard materials, has been adapted for small-scale testing of polymeric materials. Two key developments were described in this paper: (1) the cryo-solvent manipulation technique, which provided a means to transfer and deposit delicate polymer thin films, and (2) the design of an oversized locking push-to-pull device, which enabled FIB-free tensile specimen preparation and postmortem TEM analysis. A design of a vertical mount for use with instrumented nanoindenters expanded the types of experiments possible with PTP devices, including the ability to measure the glass transition temperature.

The cryo-solvent manipulation technique is not limited to PTP sample preparation. For example, using this technique it is possible to transfer microtomed films onto grids and silicon nitride windows for TEM and X-ray microscopy. While only results for monolithic polymers have been presented, the advantages of the locking PTP device testing platform may benefit more complicated polymer systems such as composites and blends. Finally, the increased tensile area of the locking PTP devices may accommodate other types of materials, such as biological materials for nanomechanical investigations that would not be possible with small commercial PTP devices.

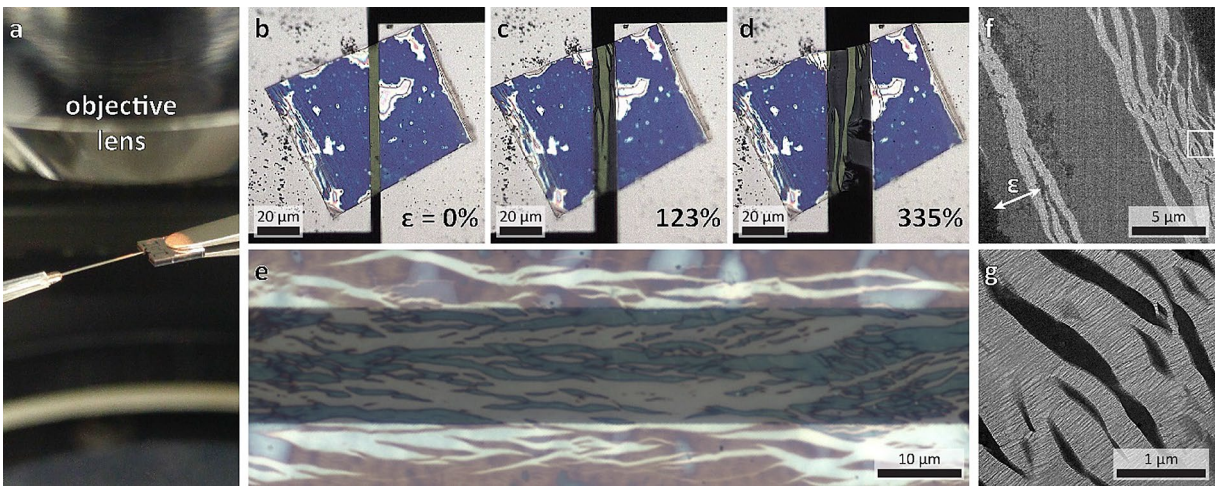

Figure 6: (a) A locking PTP device held under the objective lens of an optical microscope, about to be actuated with a micromanipulator equipped with a metal needle. (b)–(d) Video snapshots from an in situ locking PTP test of a microtomed, FIB-free film of PS (film thickness = 270 nm). The PS film reaches strains well beyond that of the bulk, as measured by the percent difference in the locking PTP gap (indicated in lower right corner of each snapshot). (e) Postmortem optical image of a microtomed, FIB-free film of PMMA on a locking PTP device with the strain-locking mechanism engaged, which provided the mechanical stability required to obtain images at this magnification (film thickness = 260 nm). (f) Low-magnification TEM overview of a microtomed, FIB-free film of PS where the edges of the locking PTP tensile gap can be seen in the upper-right and lower-left corners (film thickness = 240 nm). (g) Higher magnification of the region indicated in (f), revealing crazes not resolvable by the optical microscope. For PS, the crazing only occurred in annealed films even though both annealed and unannealed films exhibited extreme ductility [11]. Enabled by the strain-locking feature of the locking PTP device, crucial TEM imaging of the films was permitted, revealing the dependence of the deformation mode on annealing at the microstructural level.

Materials and methods

The PS used for this study was anionically polymerized (M_w = 288,800 g/mol; M_n = 274,600 g/mol; M_w/M_n = 1.05) and was purchased from Pressure Chemical (Pittsburgh, PA) and provided by The Dow Chemical Company. The elastomer used was ethylene, 1-octene and was provided by The Dow Chemical Company. The polymethylmethacrylate was purchased from Sigma-Aldrich, manufactured by Goodfellow as a cast sheet (0.5 mm thick).

Microtomy

Glass and diamond blade microtomy was used to prepare PS and PMMA specimens with thicknesses on the order of 200 nm using an RMC PowerTome XL Ultramicrotome. As the glass transition temperature, T_g, of both of these polymer glasses is well above room temperature, sectioning was performed at room temperature. A glass knife trim tool was first used to reduce the size and shape the dimensions of the blockface of a bulk sample, after which sectioning was performed using a diamond knife equipped with a reservoir filled with deionized water. This allowed the films to float along the surface of the water as they were cut. The water not only serves as a convenient way to collect the floating specimens, but also reduces compression during sectioning to yield a more uniform thickness. Using a single-hair tool and a loop tool, the films can be retrieved and deposited onto an intermediate substrate. Filter paper was used to blot the water away from the loop tool when depositing the films onto this substrate. It is important that the films did not adhere to the intermediate substrate too strongly. To accomplish this, a silicon wafer that was first roughened with high grit sandpaper was used. This reduced the contact area between the polymer films and the substrate, lowering the adhesion and allowing them to be removed without damage. Success was also achieved using filter paper or "frosted" glass slides as intermediate substrates. Films less than 100 nm in thickness required a rougher substrate, as they tended to conform to the scratches on the surface and adhered more strongly than their thicker counterparts.

Cryo-solvent manipulation

Utilizing solvents at cryogenic temperatures provides a means to manipulate the fragile films and deposit them onto the PTP device (or any substrate). Three solvents were evaluated: ethanol, methanol, and isopropyl alcohol (IPA). These solvents were chosen because they were easily obtainable and incompatible with PS and PMMA. When the cryo-chamber was set to – 165 °C, the methanol and IPA would quickly become solid and unusable. Ethanol, however, became a very viscous liquid, similar to the viscosity of honey at room temperature and is also very sticky. The viscous ethanol enabled the pickup and transfer of delicate specimens with accurate deposition onto the PTP device.

After preparing an intermediate substrate with several films deposited, it was placed into the microtome cryo-chamber and cooled to the desired temperature (depending on the solvent used). The intermediate substrate was fixed onto the knife holder by using double-sided tape which was compatible with cryogenic temperatures. The cryo-solvent manipulation was performed by first applying a small amount of solvent on the roughened intermediate substrate nearby the deposited films and a PTP device is placed on top in order to immobilize it during deposition (otherwise the PTP may cling to the single-hair tool). A smaller amount of solvent was then applied to the tensile region of a PTP device. For the oversized locking PTP devices, only enough solvent to cover the tensile region was used, as excess solvent may cause the film drift out of position during the final warm-up step. The tip of a single-hair tool was then dipped into a blob of solvent so that it was lightly coated. The sticky tip of the single-hair tool was then used to gently pick up a film from the roughened substrate, preferably at the corner of the film (Fig. 7a, Video S2). The film, attached to the end of the single-hair tool, was gently placed onto the small dab of solvent previously applied to the tensile region. The film was released from the single-hair tool as it was pulled away since the contact area between the film and the dab of solvent on the PTP device was much larger than at the tip of the hair (Fig. 7b, Video S3). The position of the deposited films can be adjusted by elevating the temperature until the solvent melts but does not evaporate. The single-hair tool can then be used to adjust the films into the desired position (Video S4). This process can be performed by hand or by equipping a micromanipulator setup with a single-hair tool that extends into the cryo-chamber.

It was found that the thin films could also be manipulated at slightly warmer temperatures (roughly – 85 °C) at which the solvent remained in a liquid state, but low enough such that evaporation was suppressed. In this case, the same procedure as described for the viscous ethanol was used: a small amount of the solvent is painted onto a PTP device at the tensile gap and a small drop at the tip of the single-hair tool is used to pick up and deposit an individual film (Fig. 7c, d, Video S5—note here a locking PTP device was used). It was found that IPA worked best for cryo-solvent manipulation at the warmer setting. This is due to a common problem in cryo-microtomy, which is that water in the air freezes and "snows" into the cryo-chamber. The ice crystals land on the solvent in the cryo-chamber, melt and dissolve. It was observed that when ethanol was used, a critical concentration of water is reached such that the mixture freezes into a rigid solid. This creates a limited window of time in which ethanol can be

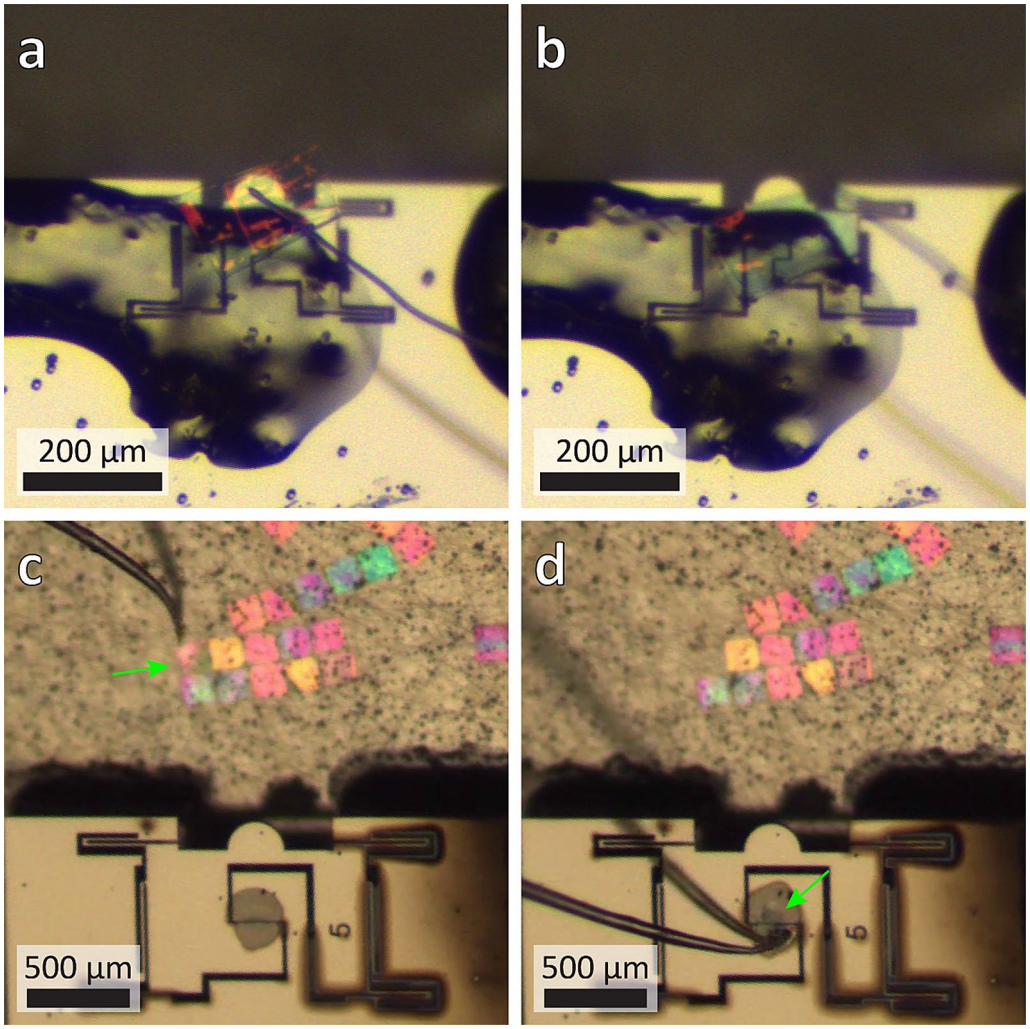

Figure 7: (a) Microtomed film of PS clinging to the end of a single-hair tool extending into the cryogenic chamber of the microtome. Below the film, a dab of viscous ethanol covers a PTP device, ready for deposition. (b) The PS film is shown deposited onto the PTP device by adhering to the viscous ethanol. Note that the film covers most of the mobile region of the device, which will require the use of a FIB to clear the trenches and shape the tensile specimen. (c) Single-hair tool picking up a microtomed film of PMMA inside the cryogenic chamber. A small amount of IPA has been applied to the tensile region of a locking PTP device. The temperature is low enough such that the solvent remains liquid but does not readily evaporate. (d) Image of the PMMA film from (c) just after deposition onto the locking PTP device by gently touching the film onto the liquid IPA previously applied to the tensile region (indicated by arrow). No FIB milling was required since the film does not extend beyond the tensile region of the locking PTP device (See SI for videos.).

used for cryo-manipulation (this can be extended by the operator wearing a mask or face covering, which reduces moisture due to respiration entering the cryo-chamber). This problem, however, was not encountered with IPA. The warmer temperature not only reduced ice formation, but when ice mixed with the IPA it did not cause it to freeze. The advantage of using viscous ethanol is that the films are easier to pick up with the single-hair tool compared to using the liquid IPA method. Additionally, if cryo-microtomy is used to prepare specimens, as required for polymers with a T_g below room temperature, the viscous ethanol could be used to transfer films directly from the knife onto a PTP device mounted just below the knife edge, thus circumventing the need for an intermediate substrate. However, due to the problems with ice formation, using IPA at roughly − 85 °C was the preferred method for preparing PTP specimens.

The final step in the sample transfer procedure is to elevate the temperature to ambient and let the solvent evaporate, leaving behind a film deposited firmly on the PTP device. Other solvents may also work, as long as the material is chemically resistant and can be wetted by the solvent.

FIB milling

The mobile region of a commercially available PTP device is about 0.7 mm^2, with a tensile gap of 2.5 µm and width of the tensile region of just under 19 µm (Fig. 1a, 3a). This width is below

the practical width of a polymer film that can be microtomed and deposited onto the device without extending beyond the tensile region, which would hinder proper actuation of the device and prevent quantitative analysis. Thus, focused ion beam (FIB) milling was used to clear the excess material and shape a tensile specimen. Using a Zeiss ORION NanoFab, milling (gallium and helium FIB) was performed blindly such that the gauge section was never imaged by the ions. This was achieved by using an optical image as a map, following the trenches of the device at a high enough magnification such that the material spanning the tensile gap was not exposed. The gallium FIB was used at higher currents (> 1 nA at 30 kV) to clear the trenches up to the tensile region, and then the helium FIB was used at a low current (10 pA at 25 kV) to shape the tensile specimen into a dogbone geometry (Fig. 2a, b). Milling at low currents increases the milling time and so sample drift becomes more problematic. To minimize the effects of drift, only the outline of the dogbone geometry was milled, one side at a time. After the outline was milled, the excess material on either side of the dogbone was cleared (Fig. 2b). Note that the dogbone geometry was determined by scaling down the dimensions of the ATSM D638 type IV specimen [20]. The width of the narrow section was doubled to increase stability of the freestanding dogbone during handling and to reduce the volume of material irradiated by the FIB.

Quantitative PTP testing

A feedback controller was used to maintain a constant displacement rate during quantitative testing, for both the instrumented nanoindenter and the indenting TEM holder. The stiffness of the PTP devices ranged from 150 to 600 N/m, depending on the size and thickness of the device. No significant hysteresis was measured when the PTP device was cycled without a specimen. The stiffness of the PTP device was either determined ahead of time or was extracted from the unloading portion of the force–displacement curve after fracture or if there was slack present in the film.

Van der Waals attraction between the film and substrate was sufficient to fix the specimen across the PTP tensile gap. Slippage was only observed when bubbles of air trapped under the film prevented proper adhesion to the PTP device. Slippage events were easily identified in the force–displacement response, as an abrupt drop in load is much more dramatic than the load drop from strain softening. Additionally, concerns of slippage could be investigated after the fact by optical microscopy in two ways: (1) the interference color of the film changes when the film detaches from the PTP device surface after dramatic slippage in which half the film is no longer attached to the PTP device, (2) by comparing optical images taken before and after straining. With that being said, even when the film did not slip strain was observed to extend beyond the PTP gap edges when air pockets were present near the tensile gap.

Any slack in the film was removed from the force–displacement curve in accordance with ATSM D638 Annex A1 (toe compensation), which is done by fitting a line to initial linear response to extrapolate the actual zero value for displacement [20]. Additionally, once the spring force constant is subtracted from the data, the load is approximately zero until the end of the slack in the film is reached, indicating the value of displacement that correlates to zero strain (useful when the initial response of the material is non-linear). More often than not, this adjustment was not needed since the films would usually lay flat across the tensile gap.

Acknowledgments

This work was supported by the Dow University Partnership Initiative Program. Work at the Molecular Foundry at Lawrence Berkeley National Laboratory was supported by the U.S. Department of Energy under Contract # DE-AC02-05CH11231. Special thanks to Sanjit Bhowmick, Senior Staff Scientist at Bruker Nano, Inc., for providing oversized PTP devices (non-locking).

Data availability

We are happy to make all of the original data available upon reasonable request.

Declarations

Conflict of interest On behalf of all authors, the corresponding author states that there is no conflict of interest.

Supplementary Information

The online version contains supplementary material available at https://doi.org/10.1557/s43578-021-00163-z.

Open Access

References

1. M.D. Uchic, D.M. Dimiduk, J.N. Florando, W.D. Nix, Sample dimensions influence strength and crystal plasticity. Science **305**(5686), 986 (2004)
2. H. Bei, S. Shim, G.M. Pharr, E.P. George, Effects of pre-strain on the compressive stress–strain response of Mo-alloy single-crystal micropillars. Acta Mater. **56**(17), 4762 (2008)
3. J. Ye, R.K. Mishra, A.M. Minor, Relating nanoscale plasticity to bulk ductility in aluminum alloys. Scr. Mater. **59**(9), 951 (2008)
4. F. Lançon, J. Ye, D. Caliste, T. Radetic, A.M. Minor, U. Dahmen, Superglide at an internal incommensurate boundary. Nano Lett. **10**(2), 695 (2010)
5. D. Kiener, C. Motz, G. Dehm, R. Pippan, Overview on established and novel FIB based miniaturized mechanical testing using in-situ SEM. Int. J. Mater. Res. **100**(8), 1074 (2009)
6. B. Wu, A. Heidelberg, J.J. Boland, Mechanical properties of ultrahigh-strength gold nanowires. Nat. Mater. **4**(7), 525 (2005)
7. W.D. Nix, Yielding and strain hardening in metallic thin films on substrates: an edge dislocation climb model. Math. Mech. Solids **14**(1–2), 207 (2009)
8. S. Orso, U.G.K. Wegst, C. Eberl, E. Arzt, Micrometer-scale tensile testing of biological attachment devices. Adv. Mater. **18**(7), 874 (2006)
9. C. Chisholm, H. Bei, M.B. Lowry, J. Oh, S.A. Syed Asif, O.L. Warren, Z.W. Shan, E.P. George, A.M. Minor, Dislocation starvation and exhaustion hardening in Mo alloy nanofibers. Acta Mater. **60**(5), 2258 (2012)
10. H. Guo, K. Chen, Y. Oh, K. Wang, C. Dejoie, S.A. SyedAsif, O.L. Warren, Z.W. Shan, J. Wu, A.M. Minor, Mechanics and dynamics of the strain-induced M1–M2 structural phase transition in individual VO2 nanowires. Nano Lett. **11**(8), 3207 (2011)
11. N.R. Velez, F.I. Allen, M.A. Jones, S. Govindjee, G.F. Meyers, A.M. Minor, Extreme ductility in freestanding polystyrene thin films. Macromolecules **53**(19), 8650 (2020)
12. F. Sun, H. Li, H. Lindberg, K. Leifer, E.K. Gamstedt, Polymer fracture and deformation during nanosectioning in an ultramicrotome. Eng. Fract. Mech. **182**, 595 (2017)
13. D.J. Wyeth, A.G. Atkins, Mixed mode fracture toughness as a separation parameter when cutting polymers. Eng. Fract. Mech. **76**(18), 2690 (2009)
14. F. Sun, E.K. Gamstedt, Homogeneous and Localized Deformation in Poly(Methyl Methacrylate) Nanocutting. Nanomanufacturing Metrol. **2**(1), 45 (2019)
15. M. Sezen, H. Plank, E. Fisslthaler, B. Chernev, A. Zankel, E. Tchernychova, A. Blümel, E.J.W. List, W. Grogger, P. Pölt, An investigation on focused electron/ion beam induced degradation mechanisms of conjugated polymers. Phys. Chem. Chem. Phys. **13**(45), 20235 (2011)
16. S. Kim, M. Jeong Park, N.P. Balsara, G. Liu, A.M. Minor, Minimization of focused ion beam damage in nanostructured polymer thin films. Ultramicroscopy **111**(3), 191 (2011)
17. F.I. Allen, N.R. Velez, R.C. Thayer, N.H. Patel, M.A. Jones, G.F. Meyers, A.M. Minor, Gallium, neon and helium focused ion beam milling of thin films demonstrated for polymeric materials: study of implantation artifacts. Nanoscale **11**(3), 1403 (2019)
18. R.F. Egerton, P. Li, M. Malac, Radiation damage in the TEM and SEM. Micron **35**(6), 399 (2004)
19. J. Rieger, The glass transition temperature of polystyrene. J. Therm. Anal. **46**(3–4), 965 (1996)
20. ASTM D638–14, Standard Test Method for Tensile Properties of Plastics, ASTM International, West Conshohocken, PA, 2014, www.astm.org